

# PRE-COMBUSTION CO<sub>2</sub> CAPTURE AT HIGH TEMPERATURE WITH ALKALINE PROMOTED ALUMINAS AND HYDROTALCITES: THE CRUCIAL ROLE OF ALKALINE CATIONS IN CO<sub>2</sub> ADSORPTION<sup>‡</sup>.

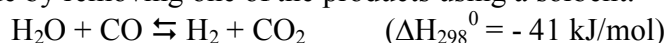
*Stéphane Walspurger* \*, Paul D. Cobden, Wim G. Haije, Ruud W. van den Brink, Hydrogen production and carbon capture, Energy research Centre of the Netherlands, Petten, Netherlands

## Abstract

Alkali promotion effects on CO<sub>2</sub> sorption have been characterised by a series of complementary analytical techniques on  $\gamma$ -alumina, magnesia, hydrotalcites and alkaline promoted corresponding materials under conditions representative for WGS conditions. Alkaline carbonates are destabilised when interacting with solid surface as evidenced by thermogravimetric analyses and temperature programmed desorption. Structural rearrangements have been observed in alkali promoted hydrotalcite at the temperature used for capture. Moreover, in the presence of CO<sub>2</sub>, the reconstruction of hydrotalcite cooled at room temperature after the experiment could not be observed most probably due to the formation of new carbonate species at high temperature that are stable while temperature decreases and prevent the reconstruction of crystalline hydrotalcite. In addition, in situ vibrational spectroscopies (Raman and DRIFT) showed that carbonates rearrange while heating and that alkali ions strongly interact with carbonate groups coordinated to aluminium oxide centres. Indeed both techniques highlight remarkably the loss of symmetry for carbonates group and comparison between parent material's fingerprints evidenced that basic (KAl<sub>n</sub>O<sub>2n</sub>/CO<sub>3</sub>)-like species play a key role in CO<sub>2</sub> fixation at 400°C.

## Introduction

Power Generation from coal with reduced CO<sub>2</sub> emissions can be achieved by using Integrated Gasification Combined Cycle (IGCC) with CO<sub>2</sub> capture and storage (CCS) in the near future. This configuration should allow the reduction of the efficiency penalty due to CO<sub>2</sub> capture and be competitive in terms of LHV efficiency with currently widespread used coal-pulverized combustion technologies.<sup>1</sup> Among pre-combustion carbon capture options, the Sorption-Enhanced Reaction Process (SERP) has attracted great interest because of the optimization of reaction yield, hydrogen purity<sup>2</sup> and CO<sub>2</sub> separation from the fuel<sup>3-5</sup>. Process simulations have shown that SERP using the pressure swing adsorption mode (PSA) has a high potential for lower efficiency penalties.<sup>6,7</sup> Gasification products mainly consist of CO which has to be converted into H<sub>2</sub> and CO<sub>2</sub> via the water-gas-shift reaction. In sorption enhanced water-gas-shift (SEWGS) the equilibrium of the reaction is shifted to the product side by removing one of the products using a sorbent.



The development of such a process has been started by Air Products in the 1990s.<sup>2</sup> Attention has been focused especially on hydrotalcites because they offer i) relatively fast reversible adsorption/desorption, ii) a stable capacity for CO<sub>2</sub> during long term cyclic experiments, iii) fairly good mechanical strength in high pressure steam and iv) there is no interaction with the physically mixed

<sup>‡</sup> Most of these results have been published in ChemSusChem, 2008, 1, 643-650

water-gas-shift catalyst.<sup>8,9</sup> Using hydrotalcites (HT) as sorbent, the process has been operated successfully at temperatures between 300 and 500°C in a PSA unit (pressure between 1 and 30 bars) on a bench scale (Single Column 2 m tall, 38 mm diameter, CACHET project) for more than 6 months at the Energy research Centre of the Netherlands.<sup>10</sup>

In parallel, investigations on HT and derivative materials are ongoing at lab scale. Despite previous studies on CO<sub>2</sub> sorption using HT-based sorbents in water-gas-shift conditions,<sup>8,9,11-13</sup> the true nature of species involved in CO<sub>2</sub> reversible adsorption at such temperatures is still not clearly identified. In particular, the present study is focused on the role of alkali promoters which have been earlier found to significantly increase the reversible CO<sub>2</sub> sorption capacity of HT.<sup>6,14-16</sup> Particularly, HT as acid-base materials<sup>17</sup> may contain sites with an optimal basic strength for CO<sub>2</sub> fixation at high temperature.

Our approach was based on a systematic comparative study of HT “parent” materials such as alumina and magnesium oxide and their potassium carbonate promoted forms. Characterization of these materials has been performed by 1) sorption experiment, 2) in situ XRD to check phase transformation and 3) by infrared spectroscopy to identify rearrangements that occur at high temperatures and the CO<sub>2</sub> adsorption mechanism.

## Results and discussions

### Reversible capacity and carbonate decomposition

Hydrotalcites used in this study have been synthesized as described earlier<sup>18</sup> and have been first calcined at 400°C, promoted by potassium carbonate by incipient wetness and then dried at 120°C. In the following discussion the material is noted as HT\*, alumina is noted as AO and magnesium oxide as MO. These materials have first been investigated for their reversible CO<sub>2</sub> adsorption in the presence of relatively high partial pressure of steam at 400°C. It was found earlier that the presence of steam in the gas stream has a significant effect on the reversible CO<sub>2</sub> capacity, in the case of HT.<sup>13,19,20</sup> Increasing the steam/CO<sub>2</sub> ratio facilitates a quick and efficient desorption and has a positive influence on adsorption capacity as demonstrated recently.<sup>20</sup>

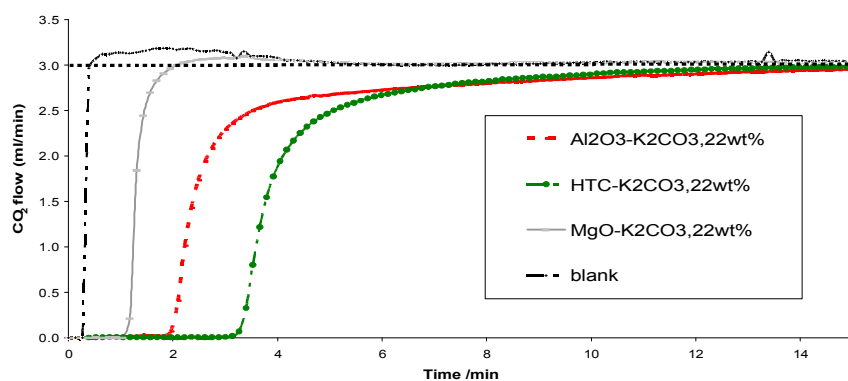


Figure 1: CO<sub>2</sub> breakthrough curves in sorption capacity measurement using 5.8% CO<sub>2</sub>, 10.7% H<sub>2</sub>O, N<sub>2</sub> balance as gas feed for adsorption step at 400°C, 1 bar. (black) blank, (grey) K<sub>22</sub>MO, (red) K<sub>22</sub>AO, and (green) K<sub>22</sub>HT\*.

Figure 1 shows the typical breakthrough curves for various potassium carbonate loaded materials. Reversible capacities for other materials have been measured using the same method and the results after the third cycle are presented together with nitrogen sorption results in table 1. It is worth to note that generally there was only a very small difference between the 2<sup>nd</sup> and 3<sup>rd</sup> cycles and longer tests carried out for some of these materials have confirmed that capacity does not vary significantly after

the 3<sup>rd</sup> cycle under these conditions. Obviously modification by potassium carbonate strongly enhances CO<sub>2</sub> capacity of HT\* as demonstrated earlier.<sup>13</sup>

**Table 1: CO<sub>2</sub> reversible sorption capacities for hydrotalcite, potassium carbonate promoted hydrotalcites and other selected materials measured after 3 cycles and their specific surface area.**

Sample	K <sub>2</sub> CO <sub>3</sub> loading (weight%)	BET Specific Surface Area (m <sup>2</sup> /g)	CO <sub>2</sub> reversible sorption capacity (mmol/g) at 400°C
K <sub>0</sub> HT*	0	48	0.06
K <sub>5</sub> HT*	5	41	0.19
K <sub>11</sub> HT*	11	40	0.30
K <sub>22</sub> HT*	22	18	0.37
K <sub>0</sub> AO	0	256	0
K <sub>5</sub> AO	5	-	0.01
K <sub>11</sub> AO	11	-	0.07
K <sub>22</sub> AO	22	113	0.27
K <sub>44</sub> AO	44	-	0.26
K <sub>0</sub> MO	0	86	0
K <sub>22</sub> MO	22	6	0.06

These experiments confirm that there exists an optimal loading of K<sub>2</sub>CO<sub>3</sub> on hydrotalcites and that the surface area drops dramatically at high loading.<sup>21</sup> The same conclusion could be drawn from the results obtained with promoted aluminas. Although unpromoted  $\gamma$ -alumina did not show any affinity for CO<sub>2</sub> under the experimental conditions, it clearly appeared that potassium carbonate promotion allows CO<sub>2</sub> fixation despite a pronounced drop in specific surface area. Lower surface area found for high K<sub>2</sub>CO<sub>3</sub> loadings are most probably caused by pore or surface blockage due to the formation of bulk K<sub>2</sub>CO<sub>3</sub> aggregates as evidenced by the SEM photos (figure 2).

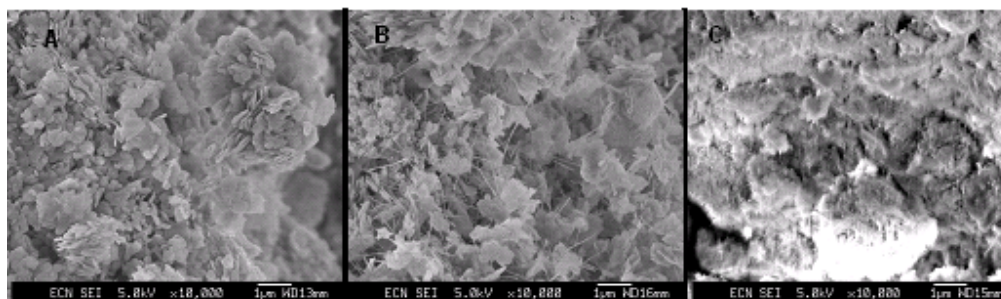


**Figure 2: SEM picture of unpromoted HT (A), 22wt% K<sub>2</sub>CO<sub>3</sub> promoted HT (B) and 22wt% K<sub>2</sub>CO<sub>3</sub> promoted  $\gamma$ -alumina (C)**

The typical platelets-like HT particles of the initial material are partially covered by some needle shaped material after potassium carbonate impregnation. In full agreement with the recent contribution of Rodrigues et al. on potassium modified HY,<sup>22</sup> small needle shaped material can also be clearly seen on  $\gamma$ -alumina surface. Although EDX analysis did not allow a definitive answer, it may be assumed that the needles are hydrates of potassium carbonate.<sup>23</sup> It is clear that at least part of the material deposited on the surface is responsible for the increased CO<sub>2</sub> sorption capacities for all those materials. In contrast, it has to be mentioned that commercial bulk potassium carbonate as well as magnesium oxide and other magnesium oxide precursors (Brucite and hydromagnesite) did not show any CO<sub>2</sub> reversible adsorption capacity under the experimental conditions used. Moreover potassium carbonate promoted magnesium oxide showed only a very low reversible CO<sub>2</sub> adsorption capacity compared to the promoted aluminium oxide based materials. Hence it seems that the interaction between  $\gamma$ -alumina

surface or aluminium oxide centres and potassium carbonate does play a key role in the formation of sites<sup>24-26</sup> that do actively and reversibly fix carbon dioxide under the experimental conditions used (1bar- about 60mbar CO<sub>2</sub>).

Temperature programmed desorption was carried out to analyse the decomposition of carbonates for various samples. The released CO<sub>2</sub> was analysed by mass spectrometer for HT and aluminas with increasing potassium carbonate loadings and for a potassium carbonate promoted magnesium oxide (Figure 3).

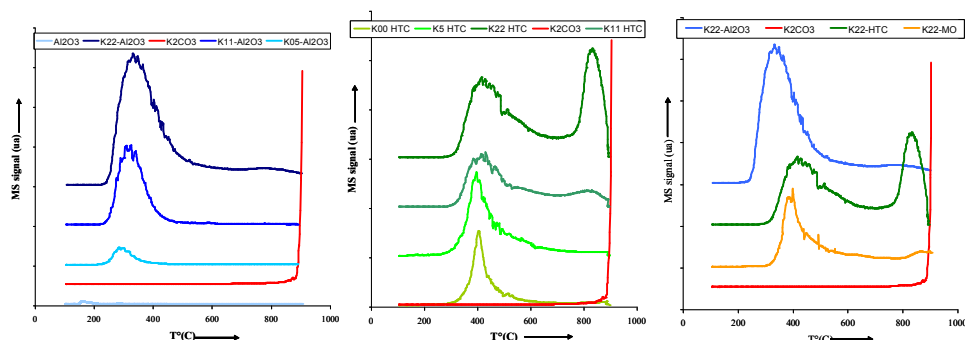


**Figure 3: Temperature programmed desorption of CO<sub>2</sub> for K<sub>0</sub>AO, K<sub>5</sub>AO, K<sub>11</sub>AO, K<sub>22</sub>AO on the left graph, K<sub>0</sub>HT\*, K<sub>5</sub>HT\*, K<sub>11</sub>HT\*, K<sub>22</sub>HT\* on the center graph and K<sub>22</sub>AO, K<sub>22</sub>MO, K<sub>22</sub>HT\* on the right graph, the red line corresponds to the TPD curve of K<sub>2</sub>CO<sub>3</sub> bulk.**

For unpromoted HT the desorption profile under standard conditions (heating in a flow of nitrogen (50ml/min) to 900°C at a rate of 10°C min<sup>-1</sup>) showed a maximum at about 400°C with a rather narrow shape although a small tail was present at higher temperature denoting carbonates decomposing at higher temperature. Although the curve was clearly broadened due to the higher concentration of carbonate in the HT promoted with 5wt% potassium carbonate, the decomposition temperature peak was not shifted towards higher temperatures. More interestingly, with higher loadings the maximum of the decomposition peak shifted toward higher temperature while its profile was significantly broadened. Note that with 22 wt% K<sub>2</sub>CO<sub>3</sub>, a significant second CO<sub>2</sub> peak was observed at 830°C probably due to the presence of bulk carbonate at the surface of the mixed oxide (originally HT). Although commercial bulk potassium carbonate started decomposing above 900°C under these experimental conditions, it can be assumed that bulk potassium carbonate deposited on the surface of the solid (as observed by SEM) is responsible for the CO<sub>2</sub> release at such a high temperature. The corresponding experiments on  $\gamma$ -alumina and promoted  $\gamma$ -alumina are depicted at the left-side of figure 3. As expected unpromoted  $\gamma$ -alumina did not show any carbonate decomposition at high temperature and only a minor amount of residual CO<sub>2</sub> is desorbed between 100 and 200°C. Increasing the amount of potassium carbonate on the surface led to an increasing amount of CO<sub>2</sub> release between 250 and 450°C. Interestingly samples with increased amount of potassium carbonate showed a gradual shift for the maximum of carbonate decomposition from 290 to 335°C with a strong broadening of the temperature range at which CO<sub>2</sub> was released toward high temperatures. Furthermore the shift of the maximum decomposition peak toward higher temperature has been confirmed in extra experiments with various heating rates (not shown here). Most probably, some carbonates more strongly bonded to the surface, which are formed at higher surface coverage, may be responsible for the modification of the TPD profile.

Finally it is of the greatest interest to compare the decomposition profile for potassium carbonate impregnated on various supports, namely alumina, hydrotalcite and magnesium oxide. In comparison

to bulk potassium carbonate it is obvious that potassium carbonate impregnated on these supports undergoes a transformation that decreases the initial decomposition temperature of  $K_2CO_3$ . Apparently,  $\gamma$ -alumina can destabilize potassium carbonate to a high extent since some  $CO_2$  was already released at  $250^\circ C$ . However the results from the thermal decomposition curves can hardly be directly correlated to the reversible  $CO_2$  sorption properties shown in table 1. In other words it would be rather difficult to assign a specific group of carbonates responsible for the increased  $CO_2$  reversible capacity on the basis of carbonates decomposition.

It has to be noted that one can try to analyze the results from carbonates decomposition in terms of basic strength. Indeed  $CO_2$  as an acid probe is entrapped in carbonate form on the solid surface. The desorption of  $CO_2$  may restore the initial basic site and as a result the temperature of carbonates decomposition may reflect, to some extent, the bond strength between  $CO_2$  and the basic site, or in other words, it may give insights on the basic strength of the surface sites. Following this concept it appears from TPD profiles that the higher the carbonate loading, the more sites of higher basic strength are formed on the surface, confirming the results found by Wang et al.<sup>25,27,28</sup> It might be that a population of sites with appropriate basic strength is specifically involved in the reversible  $CO_2$  sorption at  $400^\circ C$ . In situ structural analysis and spectroscopic investigations were therefore carried out to identify rearrangements happening in the sorbent under very similar conditions.

#### Hydrotalcite structural rearrangement during $CO_2$ capture

In-situ XRD experiments with variable temperature were performed with HT and promoted HT in the presence of steam (35 mbar) with and without carbon dioxide (120 mbar) (Figure 4).

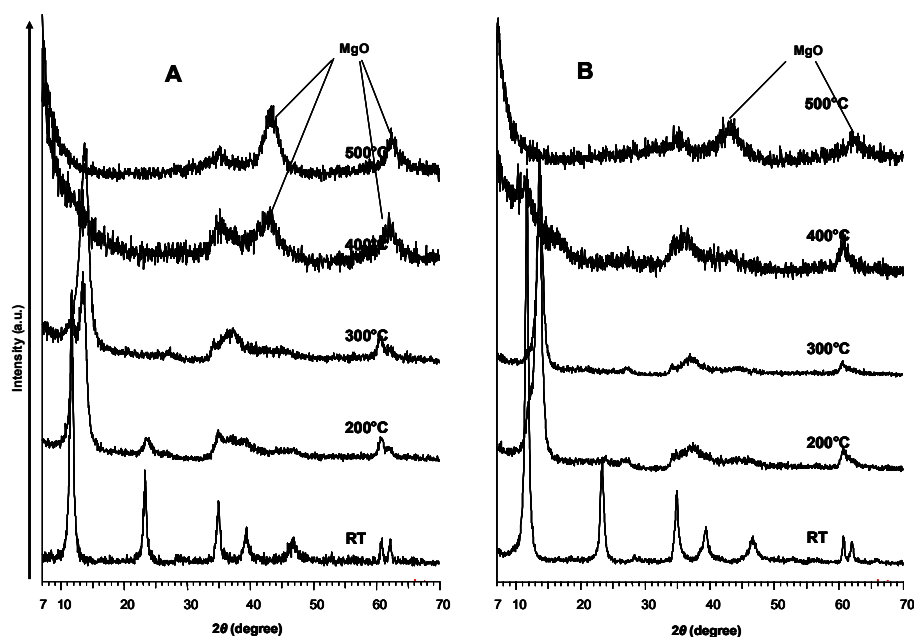


**Figure 4: In situ X-Ray powder diffractograms for  $KoHT^*$  at variable temperature in steam/nitrogen (A) and for  $KoHT^*$  at variable temperature in steam/nitrogen/ $CO_2$  (B).**

Unpromoted hydrotalcite ( $K_0HT^*$ ) and 22 wt% potassium carbonate promoted hydrotalcite ( $K_{22}HT^*$ ) were heated gradually to  $500^\circ C$  in the chosen gas stream and diffraction patterns were recorded at various temperatures. Figure 4A displays the pattern obtained for  $K_0HT^*$  in a mixture  $N_2$ /steam. Note that the diffraction patterns taken at room temperature shows the HT crystalline structure that has been reformed (reconstructed) after calcination at  $400^\circ C$  with subsequent impregnation with water at room

temperature and drying at 120°C overnight. The well known decomposition of HT crystalline phase corresponding to the collapse of the layered structure is clearly observed together with the formation of magnesium oxide crystals,<sup>29-32</sup> although neither the MgAl<sub>2</sub>O<sub>4</sub> spinel crystalline form (at high temperature) nor crystalline magnesium carbonate could be observed under these conditions.<sup>12</sup> The temperature dependence of the crystalline rearrangement was only slightly different for the other experiments. With CO<sub>2</sub> addition in the gas stream crystalline magnesium oxide appeared only at temperature above 400°C (above 300°C without CO<sub>2</sub>) for both unpromoted hydrotalcite (Figure 4B) and K<sub>2</sub>CO<sub>3</sub> promoted hydrotalcite (not shown here). In the latter case, with CO<sub>2</sub> in the stream, crystalline potassium carbonate was also observed during the experiment.

Remarkably the main differences were observed while cooling the samples to room temperature in a fixed gas stream after the heat treatment at 500°C (Figure 5). Indeed samples in permanent contact with CO<sub>2</sub> (Figures 5 B and 5 D ) did not re-crystallise to HT structure contrary to the samples that were flushed with nitrogen/steam where the memory effect of activated HT was confirmed (Figures 5 A and 5 C).

CO<sub>2</sub> might help stabilizing some carbonates species at the surface which are poorly crystalline or non-crystalline and thus it might hinder the HT re-crystallisation. In addition, it seems that potassium promoted HT is reconstructed faster than the unpromoted HT in N<sub>2</sub>/steam (figures 5A and 5C).

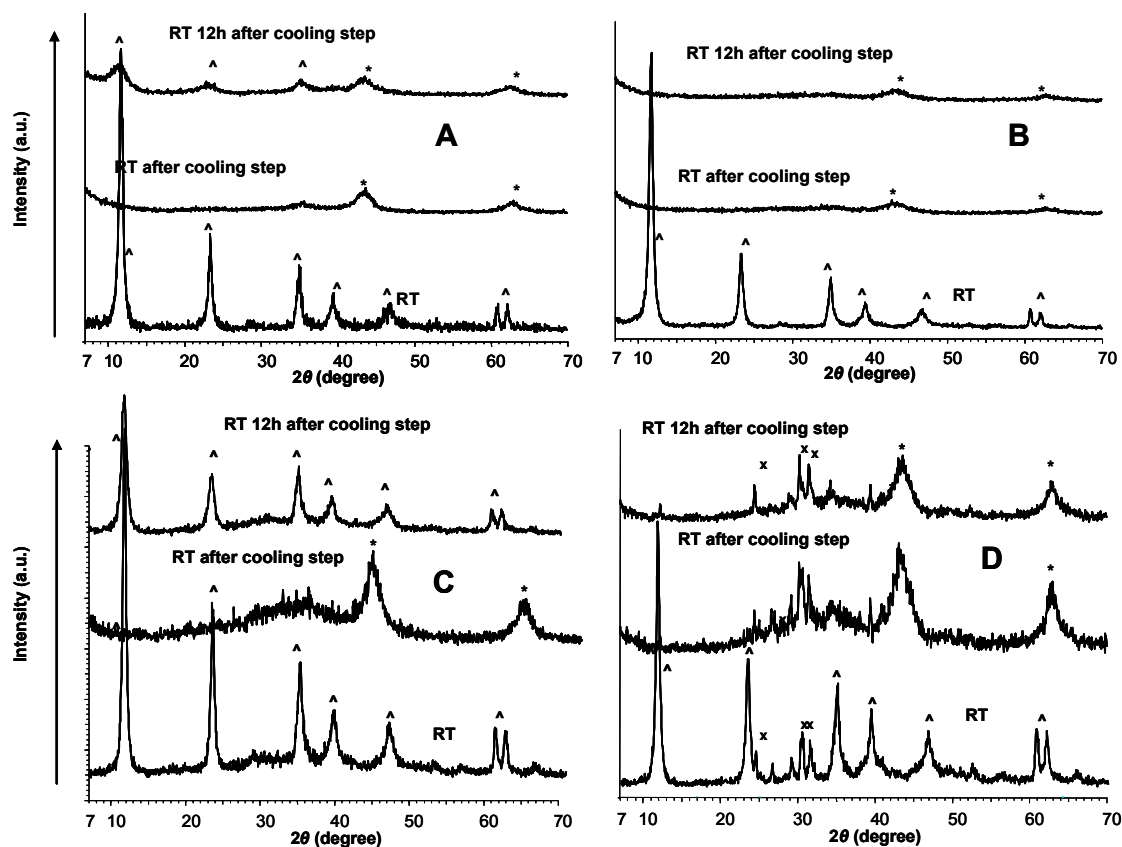


**Figure 5:** In situ X-Ray powder diffractograms for KoHT\* before heating at 500°C, after heating at 500°C and 12h after heating at 500°C flushing with water/nitrogen (A); KoHT\* before, after and 12h after experiment flushing with water/nitrogen+CO<sub>2</sub> (B); for K<sub>22</sub>HT\* before, after and 12h after experiment flushing with water/nitrogen (C); K<sub>22</sub>HT\* before, after and 12h after experiment flushing with water/nitrogen+CO<sub>2</sub> (D); Crystalline HT (^), MgO (\*) and K<sub>2</sub>CO<sub>3</sub> (x)

### Surface rearrangement during CO<sub>2</sub> capture

In-situ Diffuse Reflectance Infrared Fourier Transformed Spectroscopy (DRIFTS) study was carried out to identify the rearrangements involved in the solids at variable temperature (RT to 400°C) in the presence of N<sub>2</sub>/steam. Figure 6 shows the spectra in the 800-2000 cm<sup>-1</sup> wave numbers range obtained from unpromoted hydrotalcite, 22wt% K<sub>2</sub>CO<sub>3</sub> promoted hydrotalcite, γ-alumina and 22wt% K<sub>2</sub>CO<sub>3</sub> promoted γ-alumina respectively. Before the heat treatment, a broad absorption band is observed at 1655 cm<sup>-1</sup> for all samples which is typical of O-H bending mode from water.<sup>34-37</sup> Accordingly, this band disappears after thermal treatment at temperature between 100 and 200°C and reappeared after rehydration of the sample at room temperature (not shown here). It should be noted at this point that this band might also hint at the presence of bicarbonate species at low temperature which are known to decompose at rather low temperature.<sup>21,34</sup>

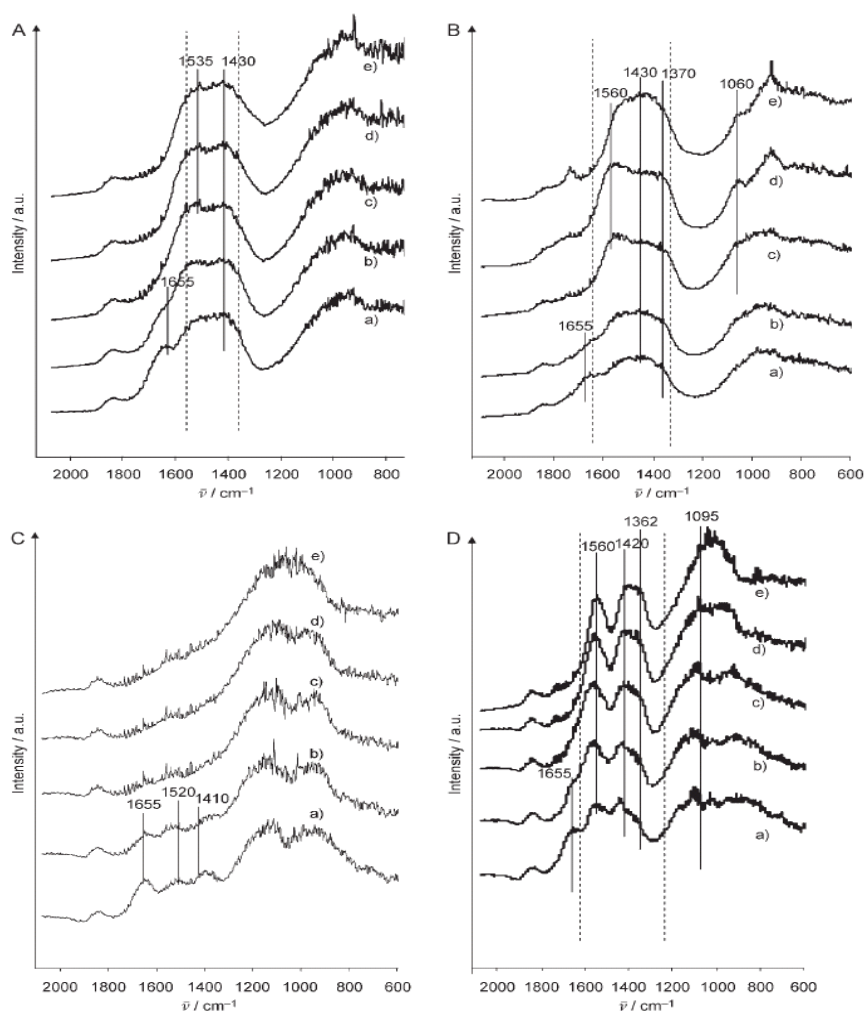


**Figure 6: DRIFT spectra of K<sub>0</sub>HT\* (A) K<sub>22</sub>HT\* (B) K<sub>0</sub>AO (C) K<sub>22</sub>AO (D) in the carbonate region at RT in N<sub>2</sub>/steam stream at room temperature (a), 100°C (b), 200°C (c), 300°C (d), 400°C (e)**

The unpromoted HT sample exhibited a strong and broad absorption band between 1400 and 1600 cm<sup>-1</sup>. When the temperature is increased there are clearly two maxima appearing at 1535 cm<sup>-1</sup> and 1430 cm<sup>-1</sup> (Figure 6A). These bands are generally assigned to  $\nu_3$  asymmetric stretching of carbonate groups.<sup>34,36-40</sup> The splitting is most probably caused by the rearrangement of surface carbonates that

involves a lowering of their symmetry. According to Busca et al.<sup>41</sup> the splitting  $\Delta\nu$   $105\text{cm}^{-1}$  can be assigned to bidentate carbonates in this case, because the polarisation might be rather low for Mg-Al atoms. For the 22 wt%  $\text{K}_2\text{CO}_3$  promoted HT (Figure 6B), band splitting also occurs when the temperature is increased. Between 200 and  $400^\circ\text{C}$  there are two broad bands peaking at  $1560$  and  $1370\text{cm}^{-1}$  corresponding to the  $\nu_3$  vibrational mode of carbonate groups. Strikingly, the splitting is increased to  $\Delta\nu$   $190\text{cm}^{-1}$  denoting a stronger perturbation of the symmetry in carbonate groups which is confirmed by the appearance of the band at  $1060\text{cm}^{-1}$ , infrared inactive for symmetric carbonates. The main reason for this significant change may be the close interaction of surface carbonates with potassium ions provided by potassium carbonates. The band at  $1430\text{cm}^{-1}$  and the weak absorption band at  $1740\text{cm}^{-1}$  maximised at  $400^\circ\text{C}$  can be unambiguously assigned to the vibration frequencies  $\nu_3$  and  $2\nu_2$  (harmonic signal of  $\nu_2$ , usually found at  $870\text{--}880\text{cm}^{-1}$ ) respectively of bulk potassium carbonate present in large amount, in agreement with the observation made by TPD and SEM<sup>42</sup>.

In contrast, experiment on non-promoted  $\gamma$ -alumina (Figure 6C) showed that no carbonates were present on the surface at high temperature. At room temperature in the presence of steam and residual  $\text{CO}_2$  from the atmosphere bands were observed at  $1655$ ,  $1520$  and  $1410\text{cm}^{-1}$  corresponding most probably to surface bicarbonates formed during the storage of the material in ambient atmosphere.<sup>43</sup>

More interestingly 22 wt%  $\text{K}_2\text{CO}_3$  promoted  $\gamma$ -alumina showed a very clear picture on rearrangement of surface carbonates occurring at elevated temperature (Figure 6D). Two bands peaking at  $1560$  and  $1362\text{cm}^{-1}$  ( $\Delta\nu$   $198\text{cm}^{-1}$ ) corresponds to  $\nu_3$  stretching frequencies for bidentate carbonates. The second band is rather large probably because of the presence of some bulk potassium carbonate with its typical single  $\nu_3$  frequency around  $1430\text{cm}^{-1}$ . Furthermore the bands broadening may be explained by the presence of K-O-(CO)-O-Al species which usually exhibit a split  $\nu_3$  frequency and  $\nu_1$  at  $1550$ ,  $1420$  and  $1095\text{cm}^{-1}$  respectively.<sup>44,45</sup> These species have previously been invoked to rationalize the enhanced basic strength of alkali promoted aluminium oxides.<sup>24,46,47</sup>

Hence the observed similarities between hydrotalcites and  $\text{K}_2\text{CO}_3$  promoted  $\gamma$ -alumina may be of the utmost importance for the comprehension of the promoting mechanism. Carbonates provided by the addition  $\text{K}_2\text{CO}_3$  are rearranged at the surface as proved by the splitting of  $\nu_3$  frequency for both materials. Moreover by comparison of the splitting values observed for promoted hydrotalcite and promoted  $\gamma$ -alumina it clearly appeared that the carbonates symmetry may be affected in a similar way. Thus it is obvious that aluminium centres play a major role in the destabilisation of potassium carbonate and may be at the origin of the increased  $\text{CO}_2$  capacity observed in our experiments at  $400^\circ\text{C}$  in agreement with previous reports.

Although Raman spectroscopy was found to be of limited help concerning HT carbonates analysis because of a pronounced fluorescence which prevents a proper analysis, the comparison between potassium bicarbonate and  $\text{K}_{22}\text{AO}$  has confirmed that  $\gamma$ -alumina destabilises potassium carbonate (figure 7).

Very interestingly, Raman spectroscopy allows to observe very clearly  $\nu_1$  stretching frequency of carbonate groups which absorb intensively in the region  $1000\text{--}1150\text{cm}^{-1}$  contrary to DRIFTS. As a reference, potassium bicarbonate shows a single absorption band at  $1027\text{cm}^{-1}$  at  $100^\circ\text{C}$ , whereas its decomposition product at  $400^\circ\text{C}$  (potassium carbonate) exhibits a band at  $1061\text{cm}^{-1}$ . Although  $\text{K}_{22}\text{AO}$  suffered from some interference due to fluorescence, two bands could be clearly detected at  $100^\circ\text{C}$ . The one around  $1060\text{cm}^{-1}$  can probably be assigned to residual bulk potassium carbonate, whereas the one around  $1094\text{cm}^{-1}$  is to be assigned to a carbonate group with a completely different symmetry. At  $400^\circ\text{C}$  it seems that both types of carbonate are still present although the relative intensity i.e. presence, obviously changed. Raman spectroscopy investigations are ongoing.



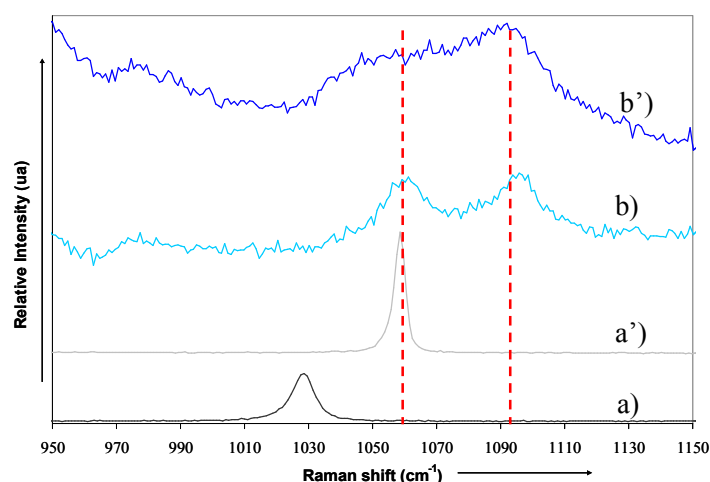


Figure 7: *in situ* Raman spectra -within 950-1150  $\text{cm}^{-1}$ - of potassium bicarbonate at 100°C (a) 400°C (a') and 22wt%  $\text{K}_2\text{CO}_3$  on  $\gamma$ -alumina at 100°C (b) and 400°C (b')

## Conclusion

Hydrotalcites, potassium carbonate promoted hydrotalcite and potassium carbonate promoted  $\gamma$ -alumina have been proved to be excellent materials for *in situ*  $\text{CO}_2$  capture during water gas shift process (SEWGS). Significant enhancement of  $\text{CO}_2$  capacity can be achieved by alkaline promotion of the sorbents. We have unambiguously demonstrated that potassium carbonate is destabilized or transformed at the surface of metal oxides and particularly  $\gamma$ -alumina and hydrotalcites. Although no new carbonates structure or species could be identified by *in situ* XRD studies we showed that fixed  $\text{CO}_2$  at 300-500°C hinders the reconstruction of hydrotalcites at room temperature most probably because of the formation of carbonate species. Moreover the *in situ* DRIFTS study confirmed that surface carbonates rearrangement occurs at high temperature and that the interaction between aluminium oxides centres and potassium carbonate plays a crucial role in the formation of active sites (strongly basic) for  $\text{CO}_2$  capture at 300-500°C. These findings are furthermore corroborated by the very low sensitivity to potassium promotion of magnesium oxide.

## References

1. F. Li, L.S. Fan, *Energy Environ. Sci.*, **2008**, *1*, 248.
2. S. Sircar, C.A.M Golden, PSA process for removal of bulk carbon dioxide from a wet high-temperature gas, US Patent 6322612, **2001**
3. IEA Prospects for  $\text{CO}_2$  Capture and Storage. International Energy Agency, Paris, **2004**.
4. B. Metz, H.C. Coninck, "CO<sub>2</sub> capture and storage: a future for coal?" ECN policy study available at <http://www.ecn.nl/publicaties/default.aspx?nr=ECN-B--07-020>
5. C. Gough, *Int. J.Greenhouse Gas Control* **2008**, *2*, 155.
6. J.R. Hufton, S. Mayorga, S. Sircar, *AIChE J.* **1999**, *45*, 248.
7. M.C. Carbo, D. Jansen, J.W. Dijkstra, R.W. van den Brink, A.H.M. Verkooijen, "Pre-combustion decarbonisation in IGCC: Abatement of both steam requirement and  $\text{CO}_2$  emissions" *ECN publication* **2007** <http://www.ecn.nl/publications/default.aspx?nr=ECN-M--07-055>
8. K.B. Lee, A. Verdooren, H.S. Caram, S. Sircar, *J. Colloid. Interf. Sci.* **2007**, *308*, 30.
9. K.B. Lee, M.G. Beaver, H.S. Caram, S. Sircar, *AIChE J.* **2007**, *53*, 2824.
10. Results to be published. Preliminary presentation at CACHET workshop available at [http://www.cachetco2.eu/publications/conf\\_pubs.html](http://www.cachetco2.eu/publications/conf_pubs.html)
11. Z. Yong, V. Mata, A.E. Rodrigues, *Ind. Eng. Chem. Res.* **2001**, *204*, 40.
12. N.D. Hutson, S.A. Speakman, E.A. Payzant, *Chem. Mater.* **2004**, *16*, 4135.

13. H.T.J. Reijers, S.E.A. Valster-Schiermeier, P.D. Cobden, R.W. van den Brink, *Ind. Eng. Chem. Res.* **2006**, *45*, 2522.
14. Y.Ding, E.Alpay, *Chem. Eng. Sci.* **2000**, *55*, 3461.
15. S. Mayorga, S. Weigel, T.R. Gaffney, J.R. Brzozowski, US Patent No 6,280,503B1 **2001**.
16. A.D. Ebner, S.P. Reynolds, J.A. Ritter, *Ind. Eng. Chem. Res.* **2006**, *45*, 6387.
17. K. Tanabe, H. Hattori, T. Yamaguchi, T. Tanaka, Acid-Base Catalysis, Proceedings of the international symposium on Acid base catalysis, Sapporo, VCH Publishers, New York, **1989**
18. F. Cavani, F. Trifirò, A. Vaccari, *Catal. Today* **1991**, *11*, 173.
19. S. Abello, J. Perez-Ramirez, *Micropor. Mesopor. Mater.* **2006**, *96*, 102.
20. M.K.R. Reddy, Z.P. Xu, G.Q. Lu, J.C. Diniz da Costa, *Ind. Eng. Chem. Res.* **2008**, *47*, 2630
21. J.I. Yang, J.N. Kim, *Korean J. Chem. Eng.* **2006**, *23*, 77.
22. E.L.G. Oliveira, C.A. Grande, A.E. Rodrigues, *J. Sep. Purif. Tech.* **2008**, *62*, 137.
23. A. Pabst, *Am. Mineral.* **1930**, *15*, 69
24. T. Horiuchi, H. Hidaka, T. Fukui, Y. Kubo, M. Horio, K. Suzuki, T. Mori, *Appl. Catal. A* **1998**, *167*, 195.
25. Y. Wang, J. H. Zhu, W. Y. Huang, *Phys. Chem. Chem. Phys.* **2001**, *3*, 2537.
26. A.G. Okunev, V.E. Sharonov, A.V. Gubar, I.G. Danilova, E.A. Paukshtis, E.M. Moroz, T.A. Kriger, V.V. Malakhov, Y.I. Aristov, *Russ. Chem. Bull. Int. Ed.* **2003**, *52*, 359.
27. Y. Wang, X.W. Han, A. Ji, L.Y. Shi, S. Hayashi, *Micropor. Mesopor. Mater.* **2005**, *77*, 139.
28. T. Yamaguchi, Y. Wang, M. Komatsu, M. Ookawa, *Catal. Surv. Japan* **2002**, *5*, 81.
29. F. Rey, V. Fornes, J.M. Rojo, *J. Chem. Soc. Faraday Trans.* **1992**, *88*, 2233.
30. M.L. Valcheva-Traykova, N.P. Davidova, A.H. Weiss, *J. Mater. Sci.* **1993**, *28*, 2157.
31. J.C.A.A. Roelofs, J.A. Bokhoven, A.J. Dillen, J.W. Geus, K.P. de Jong, *Chem. Eur. J.* **2002**, *8*, 5571.
32. T. Stanimirova,; T. Hibino, V. Balek, *J. Therm. Anal. Cal.* **2006**, *84*, 473.
33. J. Perez-Ramirez, S. Abello, N.M. van der Pers, *Chem. Eur. J.* **2007**, *13*, 870.
34. M. Del Arco, C. Martin, I. Martin, V. Rives, R. Trujillano, *Spectrochim. Acta* **1993**, *49*, 1575.
35. Y. Kim, W. Yang, P.K.T. Liu, M. Sahimi, T.T. Tsotsis, *Ind. Eng. Chem. Res.* **2004**, *43*, 4559.
36. J.T. Klopogge, The application of vibrational spectroscopy to clay minerals and layered double hydroxides, CMS workshop lectures, vol. 13, Klopogge J.T. Ed., The clay mineral society, Aurora, CO, **2005**, p.203-238.
37. R.L. Frost, B.J. Reddy, *Spectrochim Acta A* **2006**, *65*, 553.
38. T. Hibino, Y. Yamashita, K. Kosuge, A. Tsunashima, *Clays Clay Miner.* **1995**, *43*, 427.
39. F. Prinetto, G. Ghiotti, R. Durand, D. Tichit, *J. Phys. Chem. B* **2000**, *104*, 11117.
40. F. Millange, R.I. Walton, D. O'Hare, *J. Mater. Chem.* **2000**, *10*, 1713.
41. G. Busca, V. Lorenzelli, *Mater. Chem.* **1982**, *7*, 89.
42. R.A. Nyquist, R.O. Kagel, Handbook of infrared and Raman spectra of inorganic compounds and organic salts, vol. 4, Academic Press, San Diego, **1997**.
43. C. Morterra, A. Zecchina, S. Coluccia, A. Chiorino, *J. Chem. Soc. Faraday Trans.* **1977**, *73*, 1544.
44. A.S. Berger, N.P. Tomilov, I.A. Vorsina, *Russ. J. Inorg. Chem.* **1971**, *16*, 42.
45. A. Iordan, M.I. Zaki, C. Kappenstein, *J. Chem. Soc. Faraday Trans.* **1993**, *89*, 2527.
46. S.C. Lee, B.Y. Choi, T.J. Lee, C.K. Ryu, Y.S. Ahn, J.C. Kim, *Catal. Today* **2006**, *111*, 385.
47. S.C. Lee, J.C. Kim, *Catal. Surv. Asia* **2007**, *11*, 171.